

## **Titel der Förderung:**

„Maßgeschneiderte Mikroorganismen für die Produktion von Ferulasäuren als Vorstufen von hochwertigen Pflanzenprodukten“  
(FeruBase) – Teilprojekt C

**Förderkennzeichen:** 031B0836C (Fraunhofer CBP)

**Zuwendungsempfänger:** Fraunhofer-Gesellschaft zur Förderung der angewandten  
Forschung e.V., Postfach 20 07 33, 80007 München

**Ausführende Stelle:** Fraunhofer-Gesellschaft zur Förderung der angewandten  
Forschung e.V. - Fraunhofer-Zentrum für Chemisch-Biotechnologische  
Prozesse CBP, Am Haupttor Bau 1251, 06237 Leuna

**Verantwortliche Autoren:** Dr. Katja Patzsch, Sonja Höhmann

**Projektlaufzeit:** 01.02.2020 bis 31.01.2023

Das diesem Bericht zugrundeliegende Vorhaben wurde mit Mitteln des Bundesministeriums für Bildung und Forschung unter dem Förderkennzeichen 031B0836C gefördert. Die Verantwortung für den Inhalt dieser Veröffentlichung liegt bei der Autorin/beim Autor.

## TEIL I: KURZBERICHT

### Ursprüngliche Aufgabenstellung, Stand der Wissenschaft und Ablaufplan

Pflanzliche Sekundärmetaboliten, die sich von Ferulasäuren (FerA) und deren Derivaten herleiten, zeichnen sich durch eine Vielzahl an biologischen Aktivitäten aus. Sie sind unter anderem für die gesundheitsfördernde Wirkung, das Geschmacksprofil bestimmter Lebensmittel oder eine, das Altern verzögernde, Wirkung von Arzneipflanzen (z.B. *Rhodiola rosea*) verantwortlich und sind dementsprechend für eine Anwendung in der Nahrungsmittel- und pharmazeutischen Industrie attraktiv.

Heutzutage konzentriert sich die Produktion von trans-Ferulasäure hauptsächlich auf die Extraktion der Verbindung aus pflanzlichem Material wie Getreidekörnern, Reis, Weizen und Zuckerrohr oder deren Abfallströmen. Die extrahierbare Produktmenge ist jedoch gering und schwankt je nach Ausgangsmaterial und Extraktionsmethode zwischen 0,5 und 2 %. Andere, neuere Ansätze stützen sich daher auf die Verwendung von gentechnisch veränderten Mikroorganismen zur biotechnologischen Herstellung von trans-Ferulasäure unter Verwendung von Aminosäurevorläufern wie L-Tyrosin.

Das beantragte Projekt basierte auf Vorarbeiten der Verbundpartner IPB und MLU, in denen kürzlich ein FerA-produzierender *E. coli*-Stamm erzeugt werden konnte. Dieser sollte als Grundlage für die weitere Entwicklung von industriell nutzbaren Mikroorganismen zur Herstellung ökonomisch wertvoller FerAs dienen. Dazu sollten sowohl der Produktionsstamm als auch der Fermentationsprozess in einer Kooperation des Leibniz-Instituts für Pflanzenbiochemie (IPB), der Martin-Luther-Universität Halle-Wittenberg (MLU), und des Fraunhofer-Zentrums für Chemisch-Biotechnologische Prozesse (CBP) in Hinsicht auf eine wirtschaftlich tragfähige fermentative Synthese optimiert werden.

Das IPB identifizierte geeignete Enzyme zur Integration weiterführender Biosynthesewege, um die produzierten FerAs zu ausgewählten, hochpreisigen Pflanzeninhaltsstoffen von ökonomischem Interesse zu veredeln. Die Zielverbindungen umfassten dabei Flavonoide und FerA-Konjugate mit medizinischer Anwendbarkeit.

Die Optimierung der Produktionsstämme durch den MLU Partner zielte auf die Umgehung vorhandener Limitierungen der FerA-Produktion. Zum einen sollte die zelluläre Verfügbarkeit von C1-Vorläufermolekülen zur Regeneration von S-Adenosyl-Methionin (SAM) verbessert werden. Über *metabolic engineering* sollten Engpässe des Synthesewegs durch ein systematisches Screening aufgedeckt werden. Der so verbesserte Produktionsstamm sollte das derzeit nutzbare System zur Herstellung von FerA (max. bisher erreichte Konzentration: 2 g L<sup>-1</sup>) übertreffen. Die genannten Optimierungsschritte sollten in parallel verlaufenden Fermentationsversuchen durchgeführt werden, die eine direkte Skalierung in industrielle Maßstäbe erleichtert. Die, aus den Laborverfahren gewonnenen Erkenntnisse, sollten am CBP zum Scale-Up der Fermentationen in den Produktionsmaßstab verwendet werden, um die Technologie für industrielle Partner nutzbar zu machen. Zudem sollte ein nachhaltiges Verfahren für die Isolierung der hergestellten FerAs aus der Fermentationsbrühe demonstriert werden. Weiterhin sollten die Multienzymkaskaden zur FerA-Produktion in, allgemein als sicher anerkannte, Mikroorganismen (GRAS-Status) überführt werden, um Stämme für eine Zulassung in der Lebensmittelherstellung zu generieren. Die Herstellung von FerA-Derivaten die den Produktionsstamm inhibieren sollte am Fallbeispiel Coniferylalkohol untersucht werden. Dabei sollte die Wirkung einer spezifische UDP-Glucose-Glykosyltransferase (UGT) genutzt werden, um die Toxizität für den Produktionsstamm zu reduzieren.

### Wesentlichen Ergebnisse des Ferubase Projektes im Teilprojekt C

**CBP Teil (031B0836C)** Der Fermentationsprozess für die Ferulasäureproduktion wurde erfolgreich von der MLU (1 L-Maßstab) zum CBP (10 L-Maßstab) transferiert. Dabei erfolgte für das Medium eine Umstellung von Chemikalien mit Laborqualität (und hoher Reinheit) zu Chemikalien technischer Qualität. Dadurch war es möglich die Rohstoffkosten zu senken und den Prozess ökonomischer zu gestalten. Zudem wurden zuzugebenden Aminosäuren in NaOH anstatt HCl gelöst, um Abwasserrichtlinien im Großmaßstab zu erfüllen und eine Korrosion der Edelstahl-Fermenter zu verhindern. Im Anschluss an den Technologietransfer wurde der Prozess schrittweise in den 1 m<sup>3</sup>-Maßstab überführt. Hier mussten einzelne Parameter wie die Feed-Strategie, DO-Regelung und Zugabe von Antischaummittel für eine optimale und einfache Prozessführung angepasst werden. Im 10 L-Maßstab als auch im 1 m<sup>3</sup>-Maßstab konnte eine vergleichbare Produktkonzentration erreicht werden, wie im Labormaßstab bei dem Verbundpartner MLU. Zum Ende des Projektes erfolgte die Etablierung eines mehrstufigen Downstream Processing Verfahrens im Pilotmaßstab zur Aufreinigung der Ferulasäure aus der Fermentationsbrühe. Die Bilanzierung über alle Schritte ergab für das DSP eine Ausbeute von 20 %. Durch die Verwertung bzw. dem Recycling von Nebenströmen wäre es möglich die Gesamtausbeute der Ferulasäure erheblich zu steigern.

## TEIL II: EINGEHENDE DARSTELLUNG DER PROJEKTERGEBNISSE

As planned, the largest share of the funded amount was used for personnel costs. These comprised the working time of scientific personnel (working group leaders, scientists, engineers and scientific assistants) and technical personnel for carrying out experiments and setting up and converting facilities. Scientific contributions were made from:

Dr. Tino Elter  
Dr. Katja Patzsch  
M.Sc. Sonja Höhmann  
M.Sc. Niklas Grimm  
M.Sc. Leon Klose  
M.Sc. Khyati Alpesh Shah

The second largest share was spent on materials. This includes, among other things, costs for media components, sensors, septa and other wear parts, laboratory consumables, columns for analytics, and adsorbents and solvents for the purification process.

In addition, there were minor expenses for travel funds for meetings with collaborative partners and for participation in the Achema conference.

The requested personal and consumable funds were used exclusively for project-related work.

Detailed numerical evidence is presented in a separate document from the grantee.  
Scientific-technical results of the project.

The work at CBP focused on fermentative ferulic acid production on a pilot scale (up to 1 m<sup>3</sup>) and the establishment of subsequent, economical product processing (work packages C1 - 3). The results of the individual work packages are presented below.

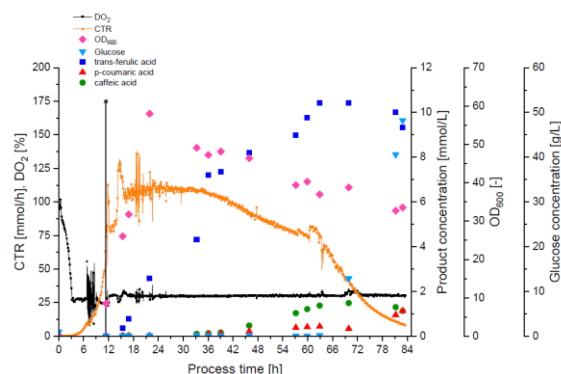
### ***AP C.1. Yield and cost-optimized fermentation process***

The aim of this work package was to increase the yield of ferulic acid concentration by adjusting various process parameters on a 1 L scale and to investigate their influence. Then the established fermentation process and the associated analytics should be transferred to CBP.

Besides downstream processing, the raw materials represent one of the largest cost factors of fermentative processes. This is particularly relevant for fermentative ferulic acid production, as the amino acids tyrosine and methionine, together with glucose, are high priced substrates. Chemicals with technical grade purity are much cheaper (tyrosine from a laboratory supplier costs about 300 €/kg; technical grade tyrosine only 16 €/kg) but have lower purity. Therefore, the influence of technical grades of media components on ferulic acid production was investigated (**Figure 1**).

It was found that about 10 mmol/L (= 1.94 g/L) of ferulic acid could be produced with both high purity chemicals and technical grade chemicals. No significant differences were found. Thus, technical grade chemicals were used for the scaling of the fermentation process.

(A) media components in laboratory grade



(B) media components in technical grade

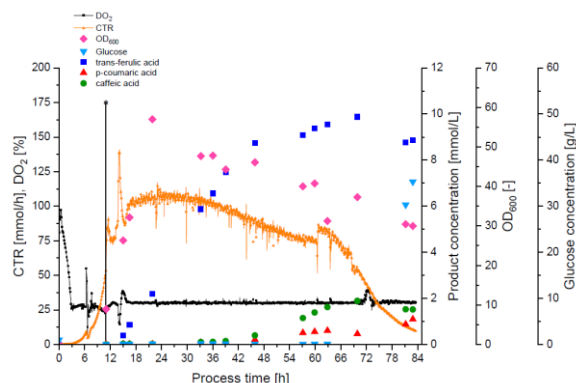


**Figure 1: Production of *trans*-ferulic acid in *E. coli* BL21  $\Delta$ tacR:Lac\_I pLysT pFA2 in 1 L scale using laboratory grade (A) and technical grade (B) chemicals.** Initial batch phase with a glucose starting concentration of 1 g L<sup>-1</sup>. After a spike in the DO signal indicating the consumption of glucose, the exponential feeding phase was adjusted to maintain the growth rate of the culture at  $\mu = 0.45$  h<sup>-1</sup>. After approximately 5 h, feeding was changed to continuous feeding. At this time, induction was also performed with 3.5 g L<sup>-1</sup> lactose (\*). 4 h after induction, the tyrosine/methionine feed was started at a rate of 1.5 mmol L<sup>-1</sup> h<sup>-1</sup> Process conditions: 37 °C; pH 7; 30 % DO.

The most important precursor of ferulic acid, the amino acid tyrosine, is only soluble to a limited extent in water, which is why tyrosine is dissolved in hydrochloric acid in the laboratory. In comparison to the 1 L laboratory reactors made of glass, industrial fermenters are made of stainless steel. Since this is susceptible to corrosion at high chloride concentrations, tyrosine was dissolved in NaOH instead of hydrochloric acid. The stability of tyrosine in the basic environment was tested and confirmed over a period of one week.

After the initial experiments in the 1-liter laboratory scale were completed and the parameters of the process were validated, the fermentation process was transferred to the 10-liter scale at CBP (Figure 2).

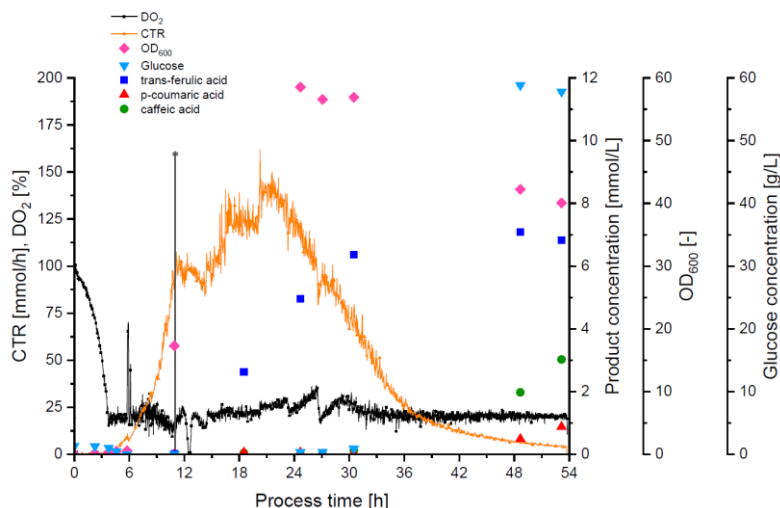


**Figure 2: Production of *trans*-ferulic acid in *E. coli* BL21  $\Delta$ tacR:Lac\_I pLysT pFA2 in 10 L-scale.** Initial batch phase with a glucose starting concentration of 1 g L<sup>-1</sup>. After a spike in the DO signal indicating the consumption of glucose, the exponential feeding phase was adjusted to maintain the growth rate of the culture at  $\mu = 0.45$  h<sup>-1</sup>. After approximately 5 h, feeding was changed to continuous feeding. At this time, induction was also performed with 3.5 g L<sup>-1</sup> lactose (\*). 4 h after induction, the tyrosine/methionine feed was started at a rate of 1.0 mmol L<sup>-1</sup> h<sup>-1</sup> Process conditions: 37 °C; pH 7; 20 % DO.

The course of the fermentation was similar to that of the 1 L fermenters. The carbon dioxide transfer rate (CTR), which can be seen as an indicator of cell viability, increased to about 100 mmol h<sup>-1</sup> at the end of the exponential feeding phase and dropped back to 90 mmol h<sup>-1</sup> shortly

after induction. This was typically followed by a short peak in the 1 L fermenters. In the 10 L fermenter, this peak was absent. Approximately two hours after induction, the CTR reached a maximum of  $130 \text{ mmol h}^{-1}$  and then steadily decreased until the end of the process. Ten hours after induction, a maximum  $\text{OD}_{600}$  of 60 was reached. This dropped to an  $\text{OD}_{600}$  of 40 by the end of the process.

The dissolved oxygen concentration was controlled at 20 %. After about 12 h, the oxygen concentration dropped to 0 %. This can be explained by the high metabolic activity of the cells after induction and was circumvented in subsequent reactor experiments by an optimized parameter setting.

Scale-up to the 10-liter bioreactor showed great similarities to the previous stage. However, the CTR dropped faster, ending the process after 54 h and yielding a lower product concentration ( $7 \text{ mmol L}^{-1}$  after 48 h). In comparison, the process time 1 L fermenter was 82 h and a final ferulic acid concentration of about  $10 - 11 \text{ mmol L}^{-1}$  was obtained. The concentration of p-coumaric acid and caffeic acid increased only at the end of the process when ferulic acid production stagnated.

In summary, raw material costs were sustainably reduced by the use of technical chemicals and the process was successfully transferred to CBP.

*The milestone CBP-MC1: "Development of the fermentation process at laboratory scale" was achieved in its entirety.*

### **AP C.2. Fermentation process in pilot scale**

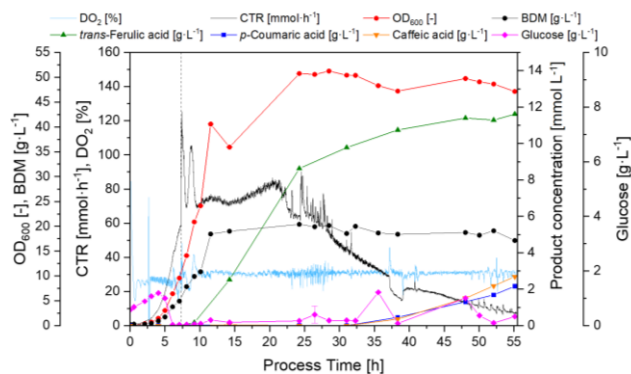
The aim of this work package AP C.2 was to transfer the developed fermentation process from laboratory to pilot scale step by step to a fermentation scale of up to  $1 \text{ m}^3$ .

For this purpose, a fermentation was first carried out on a 75-liter scale. For optimization of the fermentation process, the following adjustments were made:

- (1) Since the evaluation of the DO signal to detect the start of exponential feeding using an automated script did not work reliably in all cases, an exponential feeding profile starting immediately after inoculation was applied instead of the previously used short batch phase.
- (2) Antifoaming agent (approximately 5 mL of 1 % (w/v) PPG) was added manually prior to induction to avoid heavy foaming due to lactose addition.
- (3) The amino acid feed was decoupled from the level sensor to ensure a correct and constant substrate concentration in case of strong foam formation.
- (4) To avoid phases of oxygen limitation immediately after induction, the set point was increased from 30 % to 50 % about 30 min before induction and decreased again to 30 % about 2 h after induction.

The results of the optimized process are shown **Figure 3A**.

(A) 75 L-scale (optimized process)



(B) Amino acid and (by-) product concentration

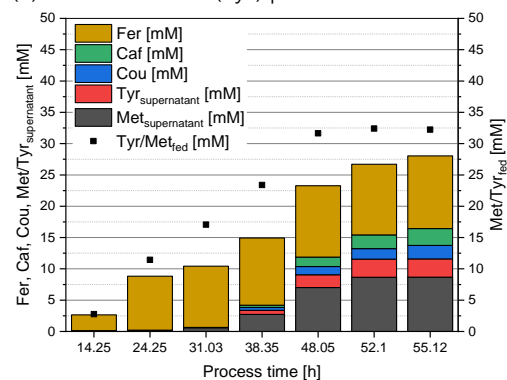


**Figure 3: Production of *trans*-ferulic acid in *E. coli* BL21  $\Delta$ tacR:Lac\_I pLysT pFA2 in 75 L scale. (A) Online and HPLC data of fermentation, (B) amino acid and (by-) product concentration in the supernatant in comparison to actual fed amount of amino acids. After inoculation an exponential feeding phase using a 50% (w/v) glucose solution was established to maintain the growth rate of the culture at  $\mu = 0.45 \text{ h}^{-1}$ . After approximately 7 h feeding was changed to a continuous feeding profile and induction was performed using  $5.5 \text{ g L}^{-1}$  lactose (dashed line). 4 h after induction, the tyrosine/methionine feed was started at a rate of  $1.0 \text{ mmol L}^{-1} \text{ h}^{-1}$  Process conditions:  $37 \text{ }^\circ\text{C}$ ; pH 7; 30 % DO.**

Scaling to the 75 L scale showed promising results, which were substantially comparable to those obtained at the 10 L scale. However, due to strong foam formation, a higher volume was measured in the tank, resulting in an increased induction with  $5.5 \text{ g L}^{-1}$  lactose instead of  $3.5 \text{ g L}^{-1}$ . The maximum  $\text{OD}_{600}$  was significantly lower than in the previous processes with an  $\text{OD}_{600}$  of about 50. Despite the misinterpretation of the level and the resulting changes in inducer concentration, a higher ferulic acid concentration ( $2.27 \text{ g L}^{-1}$  or  $11.71 \text{ mM}$  after 55 h) was achieved.

In addition, the amino acid content in the supernatant was determined (**Figure 3B**). It was noticed that the conversion of both L-methionine and L-tyrosine was very efficient within the first 30 hours of the process, as indicated by the negligibly low concentrations in the fermentation broth. In this time frame it cannot be excluded that the *trans*-ferulic acid production was limited by the availability of the precursors. In further experiments, the influence of a higher initial set point for amino acid supply could be investigated, taking advantage of the high initial productivity. After 38 h, amino acids accumulated and reached a concentration of about 8 mM for L-methionine and 2 mM for L-tyrosine. The substrate yield  $Y_{P/S}$  of the biotransformation was  $0.36 \text{ mol mol}^{-1}$ .

Following the introduction of the new production strain *E. coli* BL21  $\Delta$ R:Lacl, T7\_pFA3, RG 1 (FA3) from MLU during a project meeting, this strain was used for the following scaling experiments. This strain is capable of producing up to  $3 \text{ g L}^{-1}$  ferulic acid (Fig. 4A). Based on the previously gained experience, the fermentation process for the new strain was gradually transferred from the 1 L reactor (MLU) to the 1000 L scale (**Figure 4**).

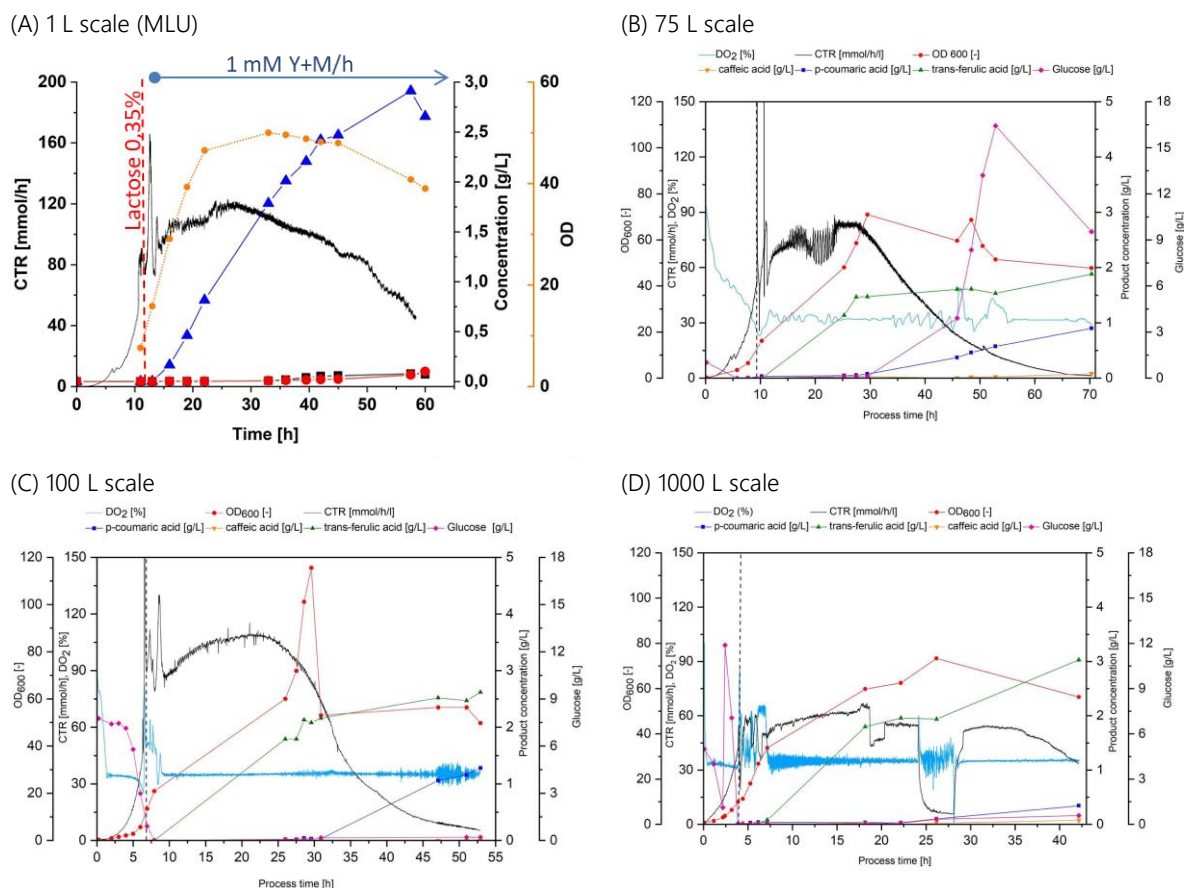


**Figure 4: Production of *trans*-ferulic acid in *E. coli* BL21  $\Delta$ R:Lacl, T7\_pFA3, RG 1 (FA3) in different scale from 1 – 1000 L.** (A/B) After inoculation an exponential feeding phase using a 50% (w/v) glucose solution was established to maintain the growth rate of the culture at  $\mu = 0.45 \text{ h}^{-1}$ . (C/D) 10 g/L glucose batch cultivation. Reaching an  $\text{OD}_{600}$  of 10, feeding was changed to a continuous feeding profile in all scales and enzyme expression for ferulic acid synthesis was induced with  $3.5 \text{ g L}^{-1}$  lactose (dashed line). The required amount of inducer was calculated based on the current volume at the time of induction. 4 h after induction, the tyrosine/methionine feed was started at a rate of  $1.0 \text{ mmol L}^{-1} \text{ h}^{-1}$ . Process conditions:  $37 \text{ }^\circ\text{C}$ ; pH 7; 30 % DO.

For cultivation on a 1000 L scale, the pre-cultivation had to be carried out in two steps: After a first preculture in a shake flask, a second preculture was inoculated in a 100 L fermenter. This was used at an  $\text{OD}_{600}$  of 5 to inoculate the 1000 L fermenter. In addition, cultivation up to induction was carried out as a (fed) batch cultivation in the 100 L and 1000 L scale. The time courses of the individual fermentations are shown in **Figure 4**.

In general, the FA3 strain behaved very similarly across the different scales. However, there were differences in respiration rates (represented by the carbon dioxide transfer rate CTR) and product concentrations. Dornheim (2021) showed that there was a relationship between the course of the CTR and the concentration of the inducer lactose. At low lactose concentrations, the CTR reaches lower values but extends longer (similar to **Figure 4A and D**), whereas at high lactose concentrations, the CTR reaches high values for a short time (similar to **Figure 4B and C**). Judging from the graphs, the 75-liter and 100-liter fermentations show signs of excessive inducer concentration. A lactose concentration of  $3.5 \text{ g L}^{-1}$  was used in all fermentations. The exact amount of lactose added to the fermenter was calculated based on the current volume. However, the different fermenters used different measurement principles to determine the volume (**Table 1**).

The volume measurement of the 1-liter and 1000-liter scales represents the most accurate measurement of liquid volume, while the 75-liter and 100-liter fermenters measure the volume of water and gas holdup. This results in higher measured volumes and therefore higher concentrations of inducer in the 75 L and 100 L scale. In addition, the CTR is calculated from the aeration rate, the CO<sub>2</sub> concentrations in the gas inlet and outlet, and the volume of the fermenter. Since the volume measurement varies in different fermenters, the absolute value of CTR is not comparable.

**Table 1 Determination of reactor volume in different scales.**

scale	measuring principle	effect
1 L	volume is determined by previously calibrated pumps	measures the volume of the liquid in the fermenter, but neglects evaporation
75 L and 100 L	potentiometric measurement	measures actual level, including foam and gas holdup
1000 L	differential pressure	measures only the liquid volume and ignores gas holdup and foam.

The product concentration in the 1-liter and 1000-liter fermenters reached about 3 g L<sup>-1</sup> ferulic acid. In contrast, the maximum ferulic acid concentration in the 75-liter and 100-liter scales reached only 2 to 2.5 g L<sup>-1</sup>, while the *p*-coumaric acid concentration was higher at about 1 g L<sup>-1</sup>.

In summary, the fermentation procedure was successfully scaled up to the 1 m<sup>3</sup> scale. In the 75 L scale, exponential feeding was applied according to the cultivation in the 1 L scale. To automate the control technology, this was carried out directly after inoculation. To simplify process control, in the 100 L and 1000 L scale, cultivation up to induction was implemented as (fed) batch cultivation. The change in feed strategy had no negative effect on the process.

*The milestone CBP-MC2: "Successful scale-up of the fermentation process" was successfully implemented.*

### AP C.3. Economic processing of FerA from the fermentation broth.

Due to the complex matrix of fermentation broths purification of desired compounds can be challenging. In the case of ferulic acid fermentation, the major challenge is to separate the intermediate products caffeic acid and *p*-coumaric acid from the product. These compounds are very similar to *trans*-ferulic acid and therefore have comparable chemical properties.

Initially, ultrafiltration followed by acidic extraction with ethyl acetate was targeted. As the project progressed, it became apparent that liquid-liquid extraction was not optimal. Due to the chemical similarity *p*-coumaric acid, caffeic acid and ferulic acid, the by-product could only be separated partially from the product using extraction. Further, it was not possible to gain a solid product after subsequent solvent evaporation, indicating high impurities. Therefore, the steps for the DSP were restructured and ultrafiltration followed by adsorption and (re)crystallization steps were applied. **Figure 5** shows the final sequence of purification steps.

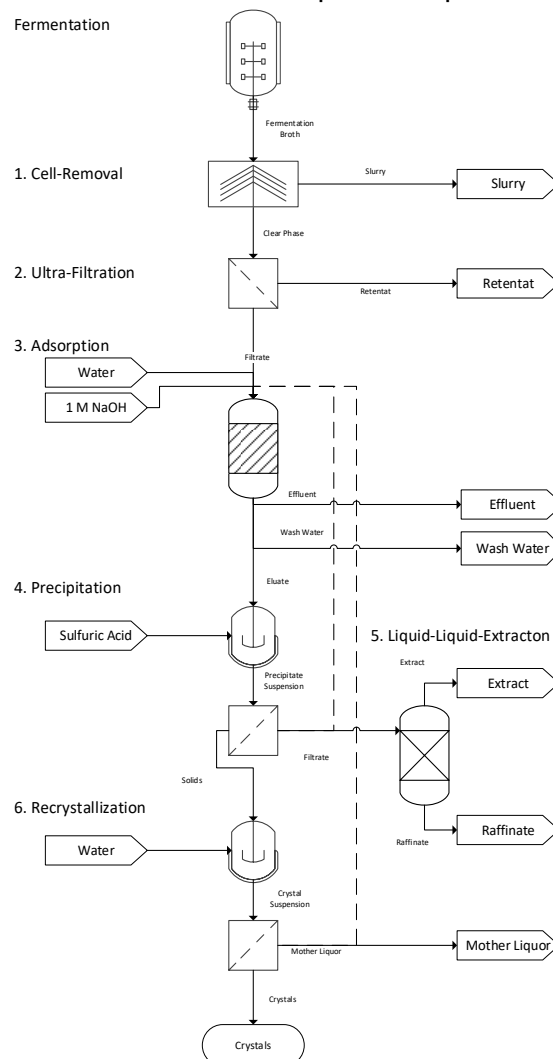


Figure 5: Overview of the final downstream process.

In the following, the separate steps of the downstream process are described in detail.

### 1. Cell separation

First, cells were removed by separation using an Alfa Laval Clara 80 disk stack separator (**Figure 6**). In one passage, 560 L of fermentation broth were separated into 500 L of clear supernatant and 60 L of cell slurry. Since the ferulic acid concentration was the same in all fractions (about 3 g/L), about 10 % of the product was lost in the slurry. This loss could be recovered by diluting the slurry with water and performing another separation step. In this case, a potential recovery of 98 % would be possible.



**Figure 6: Disk stack separator Alfa Laval Clara 80**

### 2. Ultrafiltration

In the next step, the clear phase had to be filtered by ultrafiltration to remove macromolecules such as DNA and proteins. This step was necessary because laboratory tests showed (see results under adsorption and liquid-liquid extraction) that the efficiency of the subsequent adsorption process and the phase separation of the liquid-liquid extraction were significantly improved.

The initial results in the laboratory showed that a membrane with a molecular weight cut-off (MWCO) of 10 kDa was found to be suitable to retain most of the proteins and DNA. However, dead-end filtration performed in the laboratory resulted in blockage of the membrane in some cases. Therefore, for the scale-up approach of the ultrafiltration step, a cross-flow setup was chosen and a hollow fiber module was selected due to its large surface area of 5 m<sup>2</sup> (see **Figure 7A**). The membrane was made of polyethersulfon (PES) corresponding to the material used in the laboratory scale experiments.

In a first test, the UF step was successfully demonstrated at pilot scale (75 L) with a product recovery of > 99 %.

Compared to the dead-end ultrafiltration approach used at laboratory scale, the tangential flow direction prevented clogging of the large scale filtration module. Nevertheless, an increase in permeation resistance was observed during the operation of the system, as the membrane flux decreased from the initial value of 0,27 mL cm<sup>-2</sup> h<sup>-1</sup> to 0,05 mL cm<sup>-2</sup> h<sup>-1</sup> at the end. This was most likely due to the formation of a gel layer of macromolecules on the membrane. As the formation of such a layer leads to an increase in resistance, the permeation through the membrane is reduced, prolonging the filtration process (Doran, 2013).

Since the preliminary Solid-Liquid (S/L) separation after the fermentation was only carried out by sedimentation over a period of 24 h, it can be expected that an increased release of macromolecules took place. It would therefore be advisable to investigate the performance of the filtration system after direct cell separation using a disk stack centrifuge in order to simulate a more realistic scenario for S/L-separation. In the case that the problem of a reduced flux would still be pronounced, a reduction of the transmembrane pressure could contribute to a decrease of the gel layer, as also recommended by Liu & Wang (2012). Other options would be the application of cyclic pulses in the opposite direction to the feed to reduce the layer by rapidly induced turbulence or to increase the temperature.

Nevertheless, the removal of precipitating impurities could already be observed qualitatively during the dry weight determination, as the unfiltered sample showed dark brown-black residues after evaporation compared to the filtered one (**Figure 7B**). These are most likely the result of irreversible heat denaturation of the pre-dissolved proteins and DNA. Since this phenomenon occurred only to a minor extent in the ultrafiltrated sample, it can be assumed that the targeted removal of these impurities was successful.

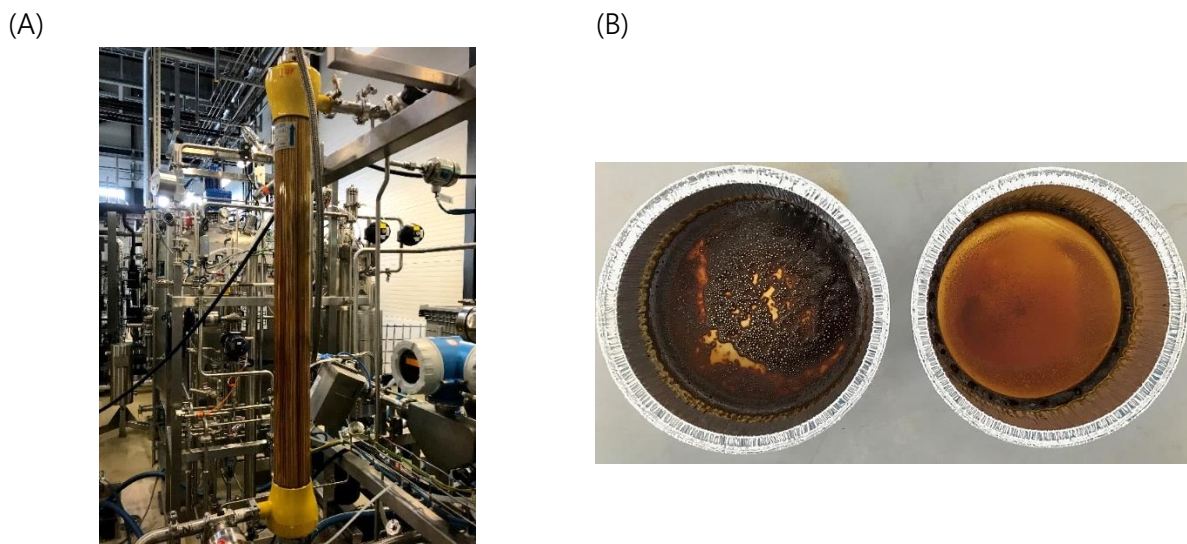


**Figure 7: (A) Hollow fiber ultrafiltration module (10 kDa MWCO) operated in cross-flow. (B) Dried fermentation broth residues before (left) and after (right) cross-flow ultrafiltration (10 kDa MWCO, 10 mL, 105 °C, 48 h).**

During a second run of the ultrafiltration for processing the fermentation broth from the 1000 L scale, the filtration had to be stopped after collecting 400 L of filtrate and 100 L of retentate due to the low flow rate. The fact that system showed low flow rates even under standard conditions with water is an indication that the membrane was blocked. Therefore, only a nominal yield of 80 % could be achieved for the ultrafiltration step from the 1000 L scale.

### 3. Adsorption

Five different adsorption materials based on hydrophobic interactions were selected and tested for their suitability for purification: Amberlite® XAD4, Amberlite® XAD16, Amberlite® XAD7HP, powdered activated carbon, granular activated carbon. First, the materials were characterized with pure, commercially available *trans*-ferulic acid at different pH values (**Figure 8A**). Afterwards, fermenter samples were used in further batch experiments to determine the material(s) with the best adsorption capabilities for the product (**Figure 8B**).

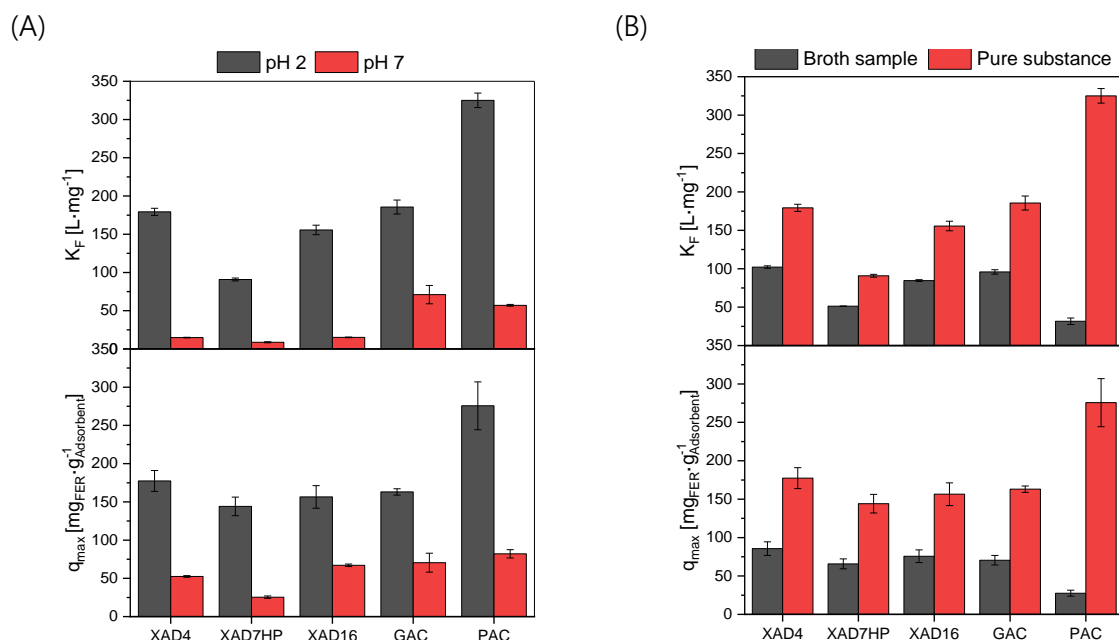


**Figure 8: Freundlich coefficients  $K_F$  and maximum loading capacity  $q_{max}$  of pure *trans*-ferulic acid at different pH values and in comparison to ultrafiltered fermentation samples. (A) Freundlich coefficients and maximum loading capacity of different adsorption materials at pH 2 and 7 for pure, commercial *trans*-ferulic acid (B) Freundlich coefficients and maximum loading capacity at pH 2 for *trans*-ferulic acid in fermentation broth in comparison to the values of the pure substance. Data were retrieved from adsorption isotherm data by non-linear fitting to the Freundlich and Langmuir adsorption models. The Freundlich coefficient  $K_F$  expresses the affinity of the *trans*-ferulic acid for the adsorbent and the capacity coefficient  $q_{max}$  from the Langmuir equation the maximum loading of the material with the product.**

The data indicated a strong influence of the pH on affinity and loading capacity for all of the five materials. As *trans*-ferulic acid is a neutral molecule at pH 2 due to the protonation of the carboxy group, the hydrophobicity of the compound is increased, allowing for better adsorption onto the materials, which rely on this kind of physicochemical interaction. In terms of the *trans*-ferulic acid affinity to the adsorbent, the activated carbons showed the highest affinity under both conditions. Concerning the influence of pH, the same trend on the affinity was also found for the capacity. Following the lower affinities obtained at pH 7, the loading was also less pronounced for all adsorbents. The highest loading capacity was found for powdered activated carbon (PAC). These findings correlate with the material properties. Having a surface area of up to 2500 m<sup>2</sup> g<sup>-1</sup>, there are far more potential adhesion sites on PAC, e.g., compared to XAD7HP, which has a surface area about 5 times smaller.

Regarding the adsorption of ultrafiltered fermentation samples, all materials showed a reduced loading capacity and the affinity for *trans*-ferulic acid towards the adsorbents in comparison to the pure substance. Impurities in the broth samples significantly affected the adhesion of the target molecule. A lower susceptibility of *trans*-ferulic acid to the adsorbent, indicates a stronger affinity for other impurities, which was also visually evident from the supernatants after the adsorption. Since both the XAD7HP and PAC samples showed strong decolorization after incubation, it can be assumed that the attachment of colored impurities to these adsorbents occurred to a greater extent than with the other three tested. To avoid negative effects on the subsequent elution of *trans*-ferulic acid, these materials were therefore excluded in further experiments. Among the materials, XAD4 was identified as the most suitable adsorbent due to its high loading capacity of 85.62 mg FerA per g adsorbent.

Finally, various washing and elution procedures were investigated to achieve the most specific and efficient recovery of *trans*-ferulic acid (**Figure 9**).

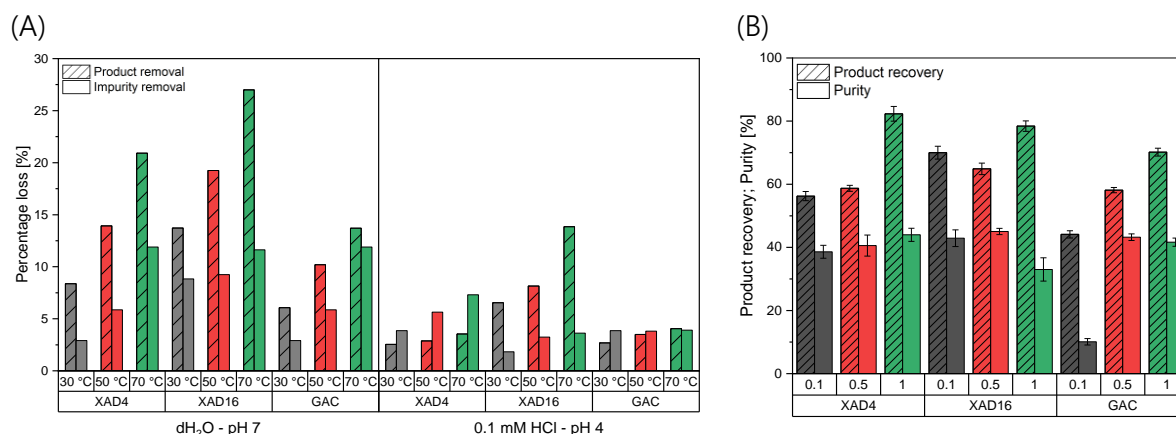


**Figure 9: Product loss and recovery after washing and elution of different adsorbent materials loaded with *trans*-ferulic acid.** (A) Product loss and removal of impurities during washing with dH<sub>2</sub>O and 0.1 mM HCl solution at different temperatures (5 h, 200 rpm). The application of higher temperatures was assumed to positively affect the desorption of only weakly bound and volatile compounds, (B) Total product recovery and purity for selected adsorbent materials after elution with differently concentration NaOH solutions (particles were washed before with 0.1 mM HCl at 30 °C, 5 h, 35 °C, 200 rpm).

The data showed that both, the temperature and pH value of the washing solution, affected the detachment of the *trans*-ferulic acid from the adsorbents. As can be seen on the left-hand side of the Fig 9A, the product loss increased strongly with rising temperatures for all of the tested materials. Compared to deionized water as a washing agent, the use of a dilute HCl solution proved to be more effective in stabilizing the adsorption of the product onto the materials, as the product loss decreased significantly. Even though only lower amounts of impurities were removed at pH 4 in comparison to pH 7, it still turned out to be the best compromise to keep product loss low. The weakly acidic washing solution resulted in less desorption of the product from the particles.

To elute the ferulic acid from the adsorber, the ferulic acid must be converted from the free acid form to the salt. By testing different NaOH concentrations for their ability to elute the product from the adsorbents (**Figure 9B**), it was found that the XAD4 and GAC particles exhibited higher product recovery with increasing NaOH concentration. With 1 M NaOH ferulic acid was eluted with a desorption efficiency or 83 % and with a purity of 44 % from XAD4.

With these results, we considered XAD4 washing with 0.1 mM HCl at 70 °C and elution with 1 M NaOH as the best option, since comparable small amounts of product were lost while still a respective number of impurities could be washed out. However, in pilot scale water had to be applied for washing to prevent corrosion of the stainless steel. The results show, that a loss of ca. 20 % of *trans*-ferulic acid will occur during the adsorption step as a consequence of incomplete desorption of the product from the adsorbent and a slight loss during particle washing.

Based on the laboratory results, for pilot scale purification, the UF filtrate was titrated to pH 2 and put into contact with Amberlite® XAD4 adsorbent in the filter dryer (**Figure 10A**). After the binding the liquid effluent was drained and the adsorber beads were washed with water to remove adhering contaminants. Upon elution with sodium hydroxide a total of 54 L of eluent containing  $13 \text{ g L}^{-1}$  of ferulic acid was collected, corresponding to a recovery of 77 % (**Figure 10B**). The adsorption step acted as a purification and concentration step, which increased the product concentration fourfold. After elution, the adsorbent beads were rinsed again with water. Depending on the design of the final process, the rinse water could be used for subsequent adsorptions, which can increase the recovery to 85 %.

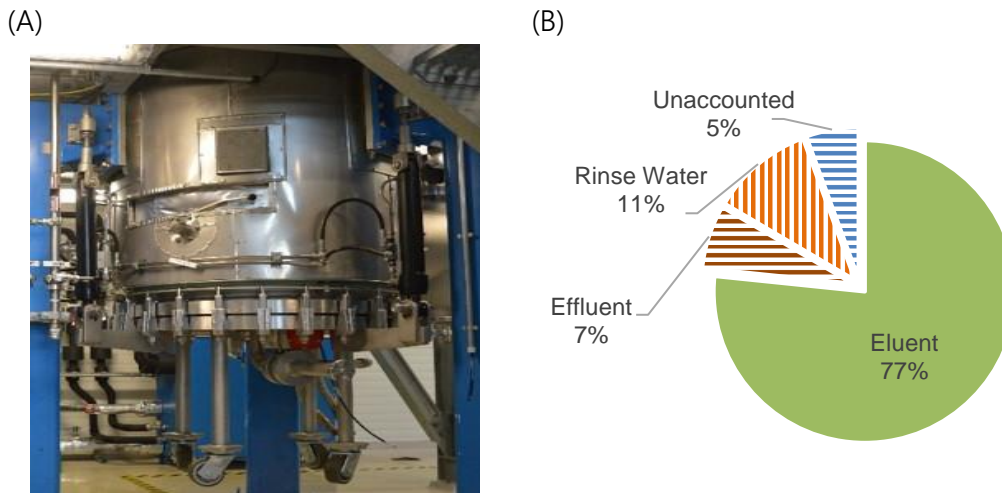


**Figure 10: (A) filter dryer (625 L) at CBP and (B) ferulic acid balance of the adsorption step with XAD4.**

#### 4. Precipitation

The solubility of ferulic acid in water depends strongly on the pH (**Figure 11**). While the solubility of ferulate is quite high at neutral conditions ( $72 \text{ g L}^{-1}$  at  $20 \text{ °C}$  and pH 7), free ferulic acid is almost insoluble at acidic conditions ( $0.7 \text{ g L}^{-1}$  at  $20 \text{ °C}$  and pH 2). This mechanism is used in the fourth purification step, in which the eluate is acidified with sulfuric acid to form an insoluble precipitate. After precipitation, the crystals are separated by filtration.

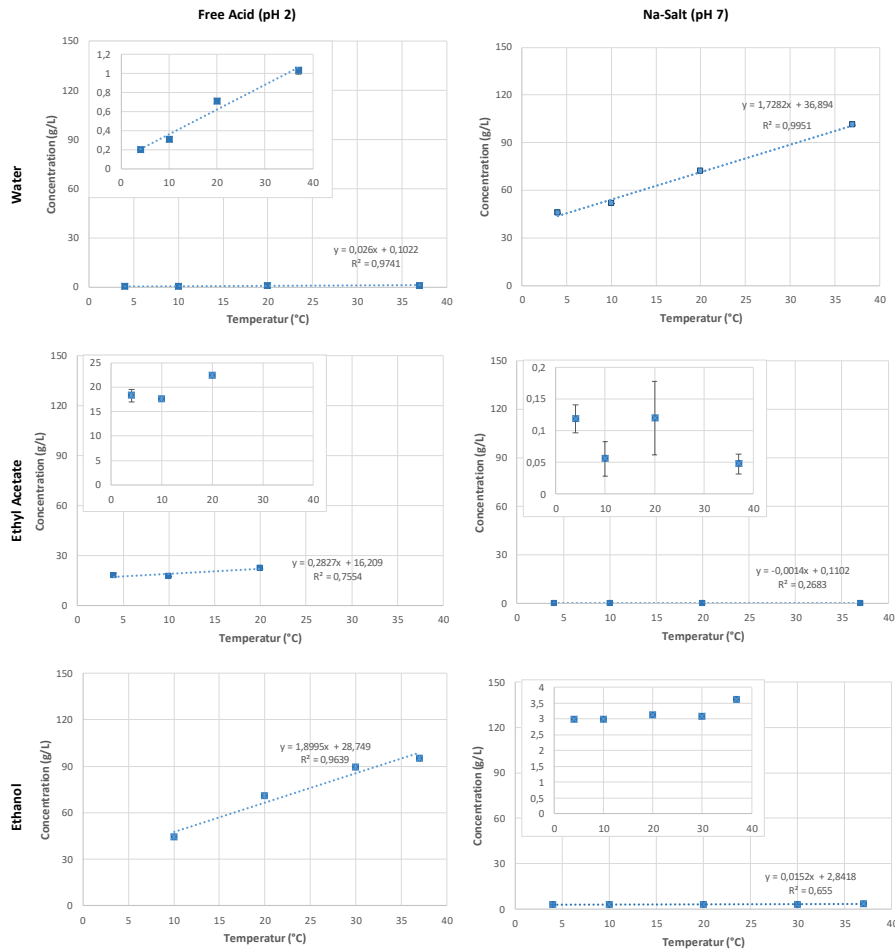
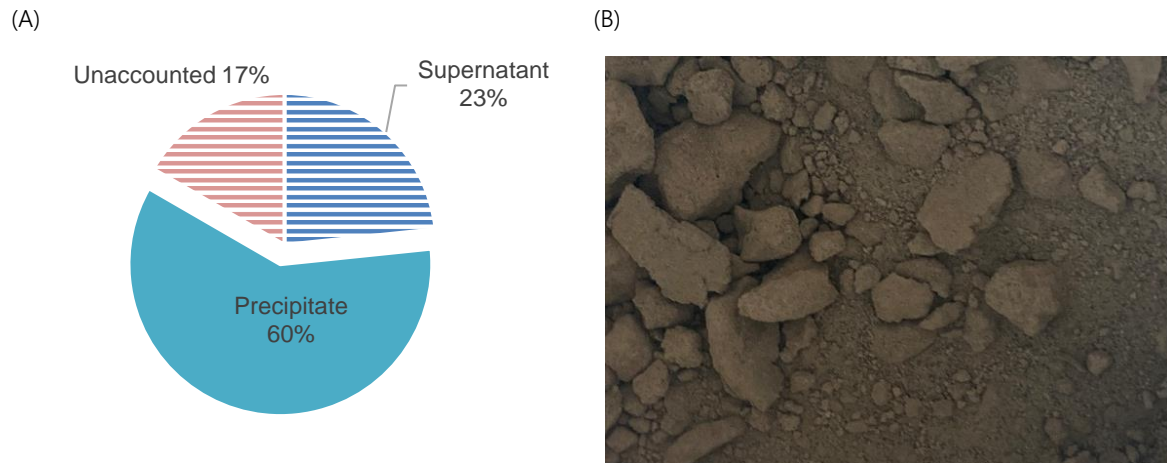


Figure 11: Solubility of ferulic acid in water, ethyl acetate and ethanol depending on pH value.

Figure 12A shows the mass balance of the ferulic acid from the precipitation step. In total, 60 % of the ferulic acid contained in the adsorbed eluate were recovered as filter cake with 40 % ferulic acid. The dried filter cake is shown in Fig. 12B. The filtrate still contains 3 g L<sup>-1</sup> FerA and could be added to the feed for the adsorption step. There is also a gap of 17 % in the mass balance, which is probably due to wall growth in the crystallizer. In the future, the residues on the wall should be redissolved in aqueous sodium hydroxide. Then, the amount of FerA on the wall can be determined and the solution can be used for further precipitation. From this, we believe that the yield of the precipitation step could be significantly improved.



**Figure 12: (A) mass balance after crystallization, (B) dried precipitate (40 % ferulic acid) after crystallization.**

### 5. Crystallization

To purify the ferulic acid from the dried precipitate two modes of crystallization were investigated: cooling crystallization in water and crystallization by evaporation in ethanol. The work in 2023 focused on how to purify ferulic acid from the dried precipitate. For those two modes of crystallization were investigated: cooling crystallization in water and crystallization by evaporation in ethanol.

Both methods have been investigated in the lab. For the demonstration in pilot scale the cooling crystallization has been selected for the following reasons:

- The cooling crystallization would not require additional process equipment.
- The mother liquor after cooling crystallization is aqueous and has a pH of 2. Thus, it could be fed back into adsorption.
- The solids gained in the precipitation step could be used in cooling crystallization without the need of drying.
- Compared to the crystallization in ethanol the crystallization in water would potentially allow for higher yields

#### Cooling Crystallization

In the pilot scale demonstration 783 g of dried containing 41.2 % of ferulic acid were suspended in 124.4 L of water and heated up to 90 °C. The suspension was incubated for 30 min and subsequently filtered through a 10 µm filter. Since there were still solid particles in the suspension, the filtration was repeated using a 1 µm filter bag. The filter cake weighed 170 g and consisted of black, coal like, amorphous particles (**Figure 13A**). The cake contained 37 g of ferulic acid or roughly 10 %. The filtrate was transferred into a crystallization vessel and cooled overnight to 8 °C. This led to the formation of crystals, which in turn were recovered using a 1 µm bag filter (**Figure 13B**). Thus, 252 g of solids were harvested. At a ferulic acid content of 87 %, 221 g FerA or 64 % the feed was recovered.

(A)

(B)

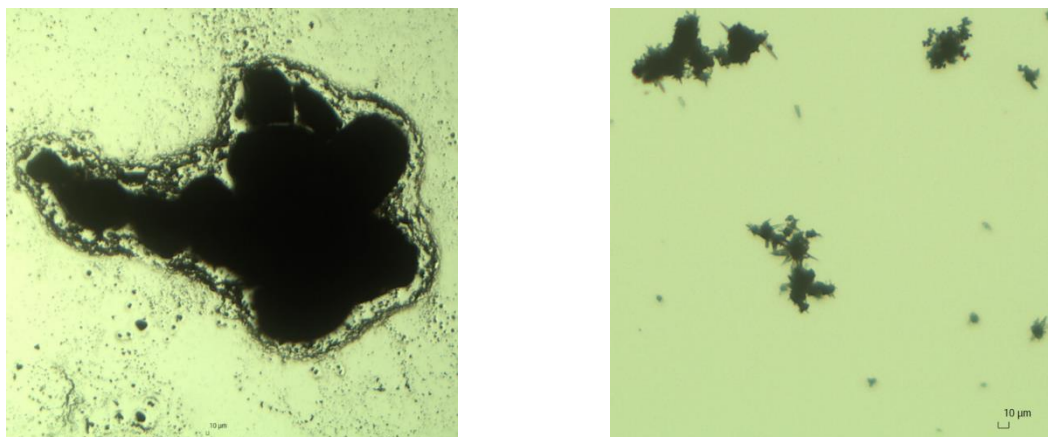


Figure 13: (A) Microscopic image of filtered solids in cooling crystallization. (B) Microscopic image of crystal suspension after cooling crystallization.

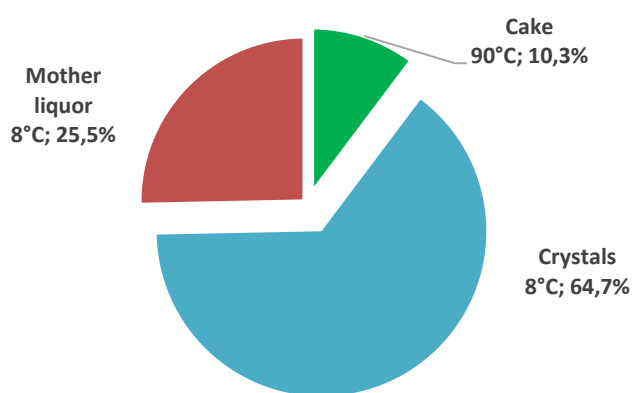


Figure 14: Ferulic acid balance of the cooling crystallization.

#### Crystallization by evaporation in ethanol

As an alternative to cooling crystallization, it was investigated, whether the dried precipitate could be dissolved in ethanol and if there is crystallization upon evaporation of the solvent.

**Figure 15** shows the solubility of pure ferulic acid in ethanol. At room temperature, one expects a maximum solubility of about 80 g/L, which is much higher than the solubility in water. Thus, a crystallization step in ethanol would require equipment with much lower volumes.

The crystallization in ethanol was carried out in lab-scale. 15 g of dried precipitate containing 5.3 g of ferulic acid were suspended in 100 mL ethanol and mixed for 1 h. The suspension was filtered through a glass fiber filter that retained 5.6 g of filter cake. The cake itself only contained 95 mg or 2 % of ferulic acid. The dark brown filtrate was filled in an open beaker with a stirring rod and was left over night to evaporate. Over the span of 30 h the volume was reduced to 27 mL. During this time crystals have formed both on the walls of the beaker and in the suspension. The suspension was filtered again and 6.6 g of crystals were harvested with a purity of 80 %. This constitutes a recovery of 44 % of ferulic acid. Despite the tar like appearance of the mother liquor, the recovered crystals were light beige (**Figure 15B**). The mother liquor still contained 67 g/L ferulic acid, which is in keeping with the solubility curve (**Figure 11**). Because of the high solubility, about 33 % of the initial ferulic acid ends up in the mother liquor (**Figure 15B**). The mother liquor might be added to a new crystallization batch; however, the concentration of impurities will increase, which might affect the crystallization behavior.

An overall mass balance revealed a gap of 14 %, which is probably due to wall growth, sampling and dilution effects.

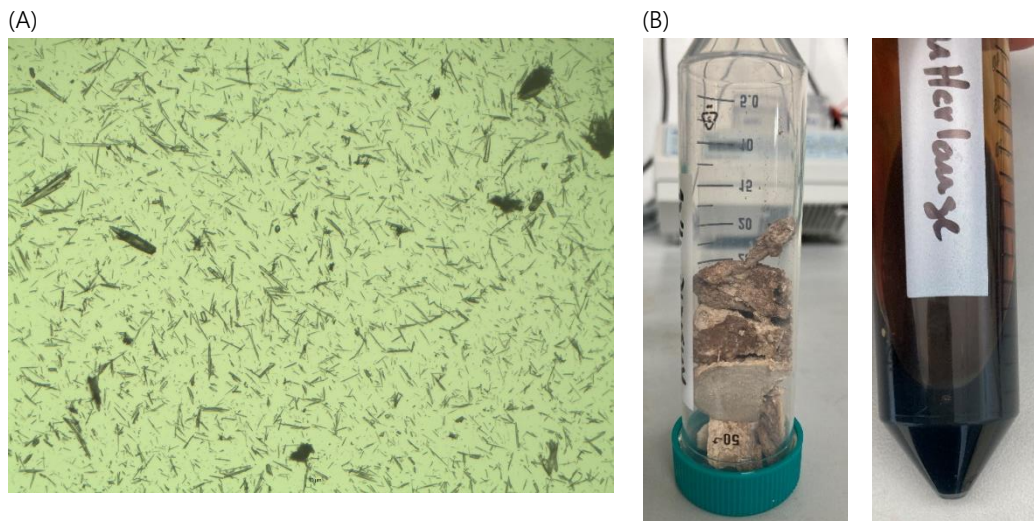


Figure 15: (A) Microscopic image of crystal suspension in ethanol. (B) Left crystals, right: mother liquor.

#### 6. Liquid-liquid extraction

In the initial downstream scheme liquid-liquid extraction was planned directly after ultrafiltration. However, due to the chemical similarity of *p*-coumaric acid, caffeic acid and ferulic acid, the by-products could only be separated partially from the product using extraction. Furthermore, after evaporation of the solvent it was neither possible to gain a solid product nor to provide a possible basis for further downstream processing step.

Nevertheless, the results shall be shortly summarized in the following as liquid-liquid extraction might be an option to used side streams.

Ultrafiltration (UF) was identified as a prerequisite for liquid-liquid extraction, as it improves phase separation (**Figure 16**). In the liquid-liquid extraction of the unfiltered culture broth, an emulsion phase formed between the aqueous and organic phases due to denaturation and precipitation of proteins and DNA. This circumstance would make a scale-up of the L/L extraction hardly feasible, as the emulsion would not allow a fast and clean phase separation, which is essential for the success of the process.

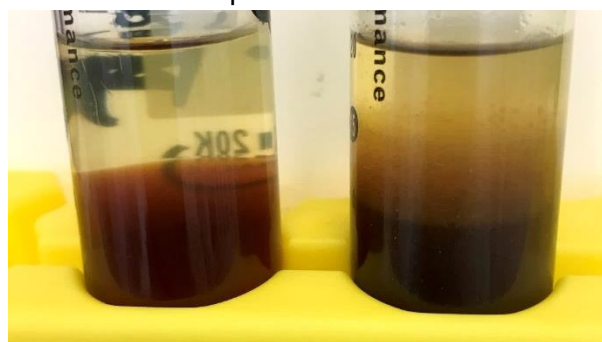


Figure 16: Comparison of phase separation during L/L-extraction of *trans*-ferulic acid from fermentation broth into EtOAc. Left: with preceding ultrafiltration. Right: without ultrafiltration

Partition coefficients were determined for *p*-coumaric acid, caffeic acid and ferulic acid and as free acid and as the respective sodium salt. The results are shown in **Table 2**.

**Table 2: Partition coefficients of hydrocinnamic acids and their respective sodium salt in one-step liquid-liquid extraction in a system with ethyl acetate:water ratio 2:1.** \*sample used from fermentation. Feed containing: 1.36 g L<sup>-1</sup> ferulic acid, 0,52 g L<sup>-1</sup> caffeic acid, and 0.18 g L<sup>-1</sup> *p*-coumaric acid.

Substance	Partition coefficient free acid, pH < 3	Partition coefficient salt form, pH 7
	$\frac{[Conc_{ethyl\ acetate}]}{[Conc_{aqueous\ phase}]}$	$\frac{[Conc_{aqueous\ phase}]}{[Conc_{ethyl\ acetate}]}$
Ferulic acid	32.8 ± 5.9	40.3 ± 16.8
Ferulic acid, fermentation sample *	25.4	
Caffeic acid	8.6 ± 5.5	24.5 ± 16.8
Caffeic acid, fermentation sample*	11.0	
<i>p</i> -Coumaric acid	43.5 ± 2.32	28.6 ± 13.6
<i>p</i> -Coumaric acid, fermentation sample*	17.4	

As expected, free acid is affine towards the organic solvent while salts favor the aqueous phase. Further, the partition coefficients are relatively high (between 10 and 40), which makes liquid-liquid extraction well suited for a first capturing step. However, the three components behave similar in terms of partition coefficients. Therefore, it is impossible to separate the three by means of extraction. Only the equilibrium for caffeic acid was lower although still being on the side of the extract. Therefore, caffeic acid can be separated from the other acids to some extent. Since caffeic acid is a toxic intermediate, reduction of this compound in the first step is attractive for easier handling.

While different combinations of extraction and precipitation worked well for purifying standard solutions of the three acids, so far, we were unsuccessful in obtaining solid ferulic acid from fermentation broth. After extraction, the extracts only have a purity between 10 to 30 %. So far, the remaining impurities have suppressed any attempt at crystallization or precipitation.

In the pilot scale demonstration only the filtrate of the precipitation step was processed by liquid-liquid extraction. Out of the 173 g of ferulic acid in the filtrate, 79 % were recovered in the extract. Afterwards, the extract was evaporated in order to increase the concentration of ferulic acid above solubility. This should facilitate crystal formation. However, this only led to the formation of stick resin. Apparently, crystallization out of ethyl acetate is difficult to reproduce. The reason for this might be that the resin phase forms a second phase during the evaporation and that ferulic acid seems to have a higher affinity to this phase. Thus, an unanticipated second liquid-liquid extraction step seems to happen.

Alternatively, the filtrate after precipitation could be fed back into the adsorption column as a feed.

### Summary

The downstream processing of ferulic acid out of fermentation broth could be successfully demonstrated in 1000 L scale. **Table 3** summarizes the process in terms of product purity and recovery. With each downstream step, the content of ferulic acid rose. The crystals after cooling crystallization and evaporation of ethanol showed a purity of over 80 % as measured by HPLC. The crystals have been sent to IPB for further analysis via NMR and LC-MS. Both measurements confirmed the measured purity. Apart from a slight contamination with coumaric acid the samples are nearly identical to the ferulic acid standard from Sigma Aldrich. Both the standards and the crystalline ferulic acid generated in this project, contained roughly 10 % of a ferulic acid isomer. In order to improve the purity and color of the product, the re-

crystallization steps could be repeated. However, it is unlikely to remove coumaric acid or isomers of ferulic acid from the crystals as these molecules are very similar to ferulic acid. Each purification step inevitably leads to a loss of product. In this first pilot scale demonstration, the total recovery was 19.5 %. The low recovery is due in large part to the fact, that side streams have not been recycled. All side streams are aqueous and could be reprocessed by adsorption. Therefore, an actual production process would yield higher recovery rates of around 73 %. The recycling of side streams has to be investigated in the future.

**Table 3 Summary downstream processing.**

Step	Sample	Caffeic acid [%]	Coumaric acid [%]	Ferulic acid [%]	Sinapinic acid [%]	Recovery [%]	Pot. Recovery [%]
Separation	Clear phase	0.1	0.5	5.1	0.1	88.5	98.0
Ultrafiltration	Permeate	0.1	0.6	5.6	0.1	81.0	98.0
Adsorption	Effluent	0.3	1.9	16.2	0.2	76.6	89.0
Precipitation	Precipitate	0.0	2.5	42.5	0.6	84.8	95.0
Recrystallization	Crystals	0.0	1.2	87.9	0.9	64.7	90.2
<b>Results</b>						<b>19.5</b>	<b>73.3</b>

In summary, the biotechnological production of ferulic acid on a pilot scale, including fermentation and product processing, was demonstrated. DSP was first tested with 75 L fermentation broth and ultimately full DSP was demonstrated with culture broth from the 1000 L fermenter.

*The milestone CBP-MC3: "Demonstration of the entire process chain on a pilot scale" was successfully implemented.*

## **References**

- Doran, Pauline M. Unit operations. Bioprocess engineering principles (2013), 1. Jg., S. 445-595 <https://doi.org/10.1016/B978-0-12-220851-5.00011-3>.
- Dornheim, Maria. (2021), Untersuchungen zur biotechnologischen Produktion von Ferula- und Sinapinsäure. Doktorarbeit. Dissertation, Halle (Saale), Martin-Luther-Universität Halle-Wittenberg, <https://doi.org/10.25673/36527>.
- Liu, S. X., & Wang, B. (2012); Purification of Ferulic Acid from Wheat by Ultrafiltration Technology. Advanced Materials Research, 524–527, 2294–2297. <https://doi.org/10.4028/www.scientific.net/AMR.524-527.2294>.